Available online at www.sciencedirect.com
SCIENCE DIRECT
Journal of Sound and Vibration 295 (2006) 436–449
JOURNAL OF SOUND AND VIBRATION
www.elsevier.com/locate/jsvi

Short Communication

On the frequency equation of a combined system consisting of a simply supported beam and in-span helical spring–mass with mass of the helical spring considered

M. Gürgöze[a,*], O. Çakar[b], S. Zeren[a]

[a]*Faculty of Mechanical Engineering, Technical University of Istanbul, Gümüşsuyu, Istanbul, 34439, Turkey*
[b]*Faculty of Engineering, University of Fırat, Elazığ, Turkey*

Received 31 March 2005; received in revised form 19 October 2005; accepted 18 January 2006

Abstract

This study is concerned with the establishment of the frequency equation of a combined system consisting of a simply supported beam and an in-span helical spring–mass, considering the mass of the helical spring. After obtaining the "exact" frequency equation of the combined system, a Dunkerley-based approximate formula is given for the fundamental frequency. The frequency equation of a simpler system is obtained as a special case. The frequency equations are then numerically solved for various combinations of the physical parameters. Calculated results are also compared with finite element solutions. Further, comparison of the results with the massless spring case reveals the fact that neglecting the mass of the spring can cause considerable errors for some combinations of the physical parameters.

1. Introduction

Various vibrating elastic systems may be modeled as Bernoulli–Euler beams to which one or several helical spring–mass systems are attached. Some of a great number of publications on this subject are given in Refs. [1–6]. The common aspect of all these works is that the mass of the helical springs is not taken into account. Although it is a well-known fact since Rayleigh that the mass of a linear spring can be taken into account approximately if one third of the spring mass is added to the mass at the end of the spring, it has been observed that the degree of the effects of the massless spring assumption on the numerical values of the eigenfrequencies in more complicated combined systems had not been investigated in the literature. As a first step to cover this gap, in Ref. [7], the frequency equation of a classical combined system is derived consisting of a cantilevered beam to the tip of which is attached a helical spring–mass system, the novelty being that the helical spring is modeled as a longitudinally vibrating elastic rod [8]. The frequency equation obtained is solved numerically for various non-dimensional mass and spring parameters. Comparison with massless spring case reveals that neglecting the mass can lead to serious errors for some parameter combinations. As an extension of this study,

*Corresponding author. Fax: +90 212 245 0795.
E-mail address: gurgozem@itu.edu.tr (M. Gürgöze).

0022-460X/$ - see front matter © 2006 Elsevier Ltd. All rights reserved.
doi:10.1016/j.jsv.2006.01.027

the present study deals with the determination of the frequency equation of a Bernoulli–Euler beam simply supported at both ends, to which is attached in-span a longitudinally vibrating elastic rod with a tip mass, representing a helical spring–mass system with mass of the helical spring considered. The principal aim is to underline once more the importance of the consideration of the mass of the helical spring for some parameter combinations and to supply the design engineers working in this area with the "exact" frequency equation of the combined system under investigation which can be thought of, for example, as a simple model of an engine elastically mounted on a structural element. Further, the frequency equation of the reduced system is established in which the free end of the longitudinally vibrating rod is fixed. Frequency equations obtained are solved for various non-dimensional mass and spring parameters and the results are compared with the massless spring case as well as with FE solutions and Dunkerley estimations. The "errors" are given, to a great extent, in graphs. It is seen that not taking into account the mass of the helical spring can lead to considerable errors for some parameter combinations.

2. Theory

2.1. Derivation of the frequency equation of the system in Fig. 1

The problem to be investigated in the present note is the natural vibration problem of the mechanical system shown in Fig. 1. It consists of a simply supported Bernoulli–Euler beam to which an axially vibrating rod with tip mass M is attached in-span. Axially vibrating rod with tip mass corresponds to a conventional helical spring–mass system. It is assumed that this combined system vibrates only in the plane of paper. The physical properties of the system are as follows: The length, mass per unit length and bending rigidity of the beam are L_1, m_1, E_1I_1 whereas the corresponding quantities and the axial rigidity of the rod are L_2, m_2, E_2A_2, respectively. It is to be noted that E_2A_2/L_2 corresponds to the spring constant of the helical spring.

The planar bending displacements in the regions to the left and right of the in-span attachment of the rod with tip mass M are denoted as $w_1(x_1,t)$ and $w_3(x_1,t)$, whereas the axial displacements of the rod are denoted as $w_2(x_2,t)$ where $x_2 = 0$ corresponds to the attachment point of the rod to the beam. $w_2(x_2, t)$ is actually a "relative" displacement of the rod, with the matching condition $w_2(0, t) = 0$. $w_1(x_1,t)$, $w_2(x_2,t)$ and $w_3(x_1,t)$ are assumed to be small.

In order to obtain the equations of motion of the system, Hamilton's principle

$$\int_{t_0}^{t_1} \delta(T - V)\,\mathrm{d}t = 0 \tag{1}$$

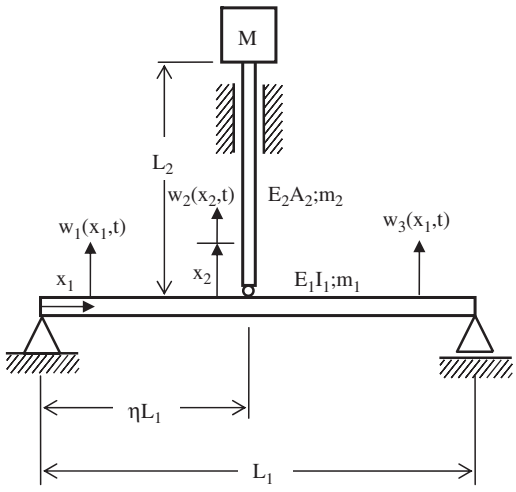

Fig. 1. Vibrational system under study: simply supported beam carrying in-span an axially vibrating rod with tip mass.

will be applied, where T and V denote the kinetic and potential energies of the system, respectively. The total kinetic energy

$$T = T_1 + T_2 + T_3 + T_4 \tag{2}$$

consists of the following parts:

$$T_1 = \frac{1}{2} m_1 \int_0^{\eta L_1} \dot{w}_1^2(x_1, t)\,\mathrm{d}x_1, \quad T_2 = \frac{1}{2} m_1 \int_{\eta L_1}^{L_1} \dot{w}_3^2(x_1, t)\,\mathrm{d}x_1, \tag{3-4}$$

$$T_3 = \frac{1}{2} m_2 \int_0^{L_2} [\dot{w}_2(x_2, t) + \dot{w}_1(\eta L_1, t)]^2\,\mathrm{d}x_2, \quad T_4 = \frac{1}{2} M[\dot{w}_1(\eta L_1, t) + \dot{w}_2(L_2, t)]^2 \tag{5-6}$$

the meanings of which are evident.

The potential energy consists of three parts, two of bending and the other due to axial displacements

$$V = V_1 + V_2 + V_3, \tag{7}$$

where

$$V_1 = \frac{1}{2} E_1 I_1 \int_0^{\eta L_1} w''^2_1(x_1, t)\,\mathrm{d}x_1, \quad V_2 = \frac{1}{2} E_1 I_1 \int_{\eta L_1}^{L_1} w''^2_3(x_1, t)\,\mathrm{d}x_1, \quad V_3 = \frac{1}{2} E_2 A_2 \int_0^{L_2} w'^2_2(x_2, t)\,\mathrm{d}x_2. \tag{8-10}$$

In the above formulations, dots and primes denote partial derivatives with respect to time t and the position co-ordinate x_1 or x_2, respectively. After putting expressions (2) to (10) into Eq. (1) and carrying out the necessary variations, the following equations of motion of the beam portions and rod are obtained:

$$E_1 I_1 w_1^{iv}(x_1, t) + m_1 \ddot{w}_1(x_1, t) = 0, \tag{11}$$

$$E_2 A_2 w_2''(x_2, t) - m_2 \ddot{w}_2(x_2, t) = m_2 \ddot{w}_1(\eta L_1, t), \tag{12}$$

$$E_1 I_1 w_3^{iv}(x_1, t) + m_1 \ddot{w}_3(x_1, t) = 0. \tag{13}$$

The corresponding boundary and matching conditions are as follows:

$$w_1(0, t) = 0, \quad w_3(L_1, t) = 0, \quad E_1 I_1 w_1''(0, t) = 0, \quad E_1 I_1 w_3''(L_1, t) = 0, \tag{14-17}$$

$$\int_0^{L_2} m_2[\ddot{w}_2(x_2, t) + \ddot{w}_1(\eta L_1, t)]\mathrm{d}x_2 + M[\ddot{w}_1(\eta L_1, t) + \ddot{w}_2(L_2, t)] - E_1 I_1 \left[w_1'''(\eta L_1, t) - w_3'''(\eta L_1, t)\right] = 0,$$

$$w_2(0, t) = 0, \quad M[\ddot{w}_1(\eta L_1, t) + \ddot{w}_2(L_2, t)] + E_2 A_2 w_2'(L_2, t) = 0, \tag{18-20}$$

$$w_1(\eta L_1, t) = w_3(\eta L_1, t), \quad w_1'(\eta L_1, t) = w_3'(\eta L_1, t), \quad w_1''(\eta L_1, t) = w_3''(\eta L_1, t). \tag{21-23}$$

Using the standard method of separation of variables, one assumes

$$w_i(x_i, t) = W_i(x_i) \cos \omega t, \quad i = 1, 2, 3 \text{ and } x_3 = x_1, \tag{24}$$

where $W_i(x_i)$ are the corresponding amplitude functions of the beam portions and the rod and ω is the unknown eigenfrequency of the combined system. Substitution of these expressions into the partial differential Eqs. (11–13) results in the following ordinary differential equations:

$$W_1^{iv}(x_1) - \beta^4 W_1(x_1) = 0, \tag{25}$$

$$W_2''(x_2) + \gamma^2 W_2(x_2) = -\gamma^2 W_1(\eta L_1), \tag{26}$$

$$W_3^{iv}(x_1) - \beta^4 W_3(x_1) = 0. \tag{27}$$

Here, the following abbreviations are introduced:

$$\beta^4 = \frac{\omega^2 m_1}{E_1 I_1}, \quad \gamma^2 = \frac{\omega^2 m_2}{E_2 A_2}. \tag{28}$$

Now, the corresponding boundary conditions are

$$W_1(0) = 0, \quad W_1''(0) = 0, \quad W_3(L_1) = 0, \quad W_3''(L_1) = 0, \tag{29-32}$$

whereas the matching conditions (18–23) give

$$m_2\omega^2 \int_0^{L_2} [W_2(x_2) + W_1(\eta L_1)]\,\mathrm{d}x_2 - M\omega^2[W_1(\eta L_1) + W_2(L_2)] + E_1 I_1 \left[W_1'''(\eta L_1) - W_3'''(\eta L_1)\right] = 0, \tag{33}$$

$$W_2(0) = 0, \quad -M\omega^2[W_1(\eta L_1) + W_2(L_2)] + E_2 A_2 W_2'(L_2) = 0, \tag{34-35}$$

$$W_1(\eta L_1) = W_3(\eta L_1), \quad W_1'(\eta L_1) = W_3'(\eta L_1), \quad W_1''(\eta L_1) = W_3''(\eta L_1). \tag{36-38}$$

Here, primes on $W_i(x_i)$ denote derivatives with respect to position co-ordinates x_i. The general solutions of the ordinary differential Eqs. (25–27) are simply

$$W_1(x_1) = C_1 \sin \beta x_1 + C_2 \cos \beta x_1 + C_3 \sinh \beta x_1 + C_4 \cosh \beta x_1, \tag{39}$$

$$W_2(x_2) = C_5 \sin \gamma x_2 + C_6 \cos \gamma x_2 - W_1(\eta L_1), \tag{40}$$

$$W_3(x_1) = C_7 \sin \beta x_1 + C_8 \cos \beta x_1 + C_9 \sinh \beta x_1 + C_{10} \cosh \beta x_1, \tag{41}$$

where C_1–C_{10} are arbitrary integration constants to be evaluated via conditions (29–38).

If these conditions are considered with Eqs. (39–41), a set of 10 homogenous equations for the unknowns C_1–C_{10} are obtained. In order to obtain nonvanishing solutions for C_1–C_{10}, the corresponding determinant of coefficients has to be equated to zero, which results in the following determinantal equation:

$$\begin{vmatrix}
0 & 1 & 0 & 1 & 0 \\
0 & 0 & 0 & 0 & 0 \\
0 & -1 & 0 & 1 & 0 \\
0 & 0 & 0 & 0 & 0 \\
-\cos \bar{\beta}\eta & \sin \bar{\beta}\eta & \cosh \bar{\beta}\eta & \sinh \bar{\beta}\eta & \frac{1}{\alpha_{22}\bar{\beta}}(1 - \cos \gamma L_2) + \alpha_M \bar{\beta} \sin \gamma L_2 \\
-\sin \bar{\beta}\eta & -\cos \bar{\beta}\eta & -\sinh \bar{\beta}\eta & -\cosh \bar{\beta}\eta & 0 \\
0 & 0 & 0 & 0 & \alpha_{11}\bar{\beta}^2 \sin \gamma L_2 - \cos \gamma L_2 \\
\sin \bar{\beta}\eta & \cos \bar{\beta}\eta & \sinh \bar{\beta}\eta & \cosh \bar{\beta}\eta & 0 \\
\cos \bar{\beta}\eta & -\sin \bar{\beta}\eta & \cosh \bar{\beta}\eta & \sinh \bar{\beta}\eta & 0 \\
-\sin \bar{\beta}\eta & -\cos \bar{\beta}\eta & \sinh \bar{\beta}\eta & \cosh \bar{\beta}\eta & 0
\end{vmatrix}$$

$$\begin{vmatrix} 0 & 0 & 0 & 0 & 0 \\ 0 & \sin\bar{\beta} & \cos\bar{\beta} & \sinh\bar{\beta} & \cosh\bar{\beta} \\ 0 & 0 & 0 & 0 & 0 \\ 0 & -\sin\bar{\beta} & -\cos\bar{\beta} & \sinh\bar{\beta} & \cosh\bar{\beta} \\ \frac{1}{\alpha_{22}\bar{\beta}}\sin\gamma L_2 + \alpha_M\bar{\beta}\cos\gamma L_2 & \cos\bar{\beta}\eta & -\sin\bar{\beta}\eta & -\cosh\bar{\beta}\eta & -\sinh\bar{\beta}\eta \\ 1 & 0 & 0 & 0 & 0 \\ \alpha_{11}\bar{\beta}^2\cos\gamma L_2 + \sin\gamma L_2 & 0 & 0 & 0 & 0 \\ 0 & -\sin\bar{\beta}\eta & -\cos\bar{\beta}\eta & -\sinh\bar{\beta}\eta & -\cosh\bar{\beta}\eta \\ 0 & -\cos\bar{\beta}\eta & \sin\bar{\beta}\eta & -\cosh\bar{\beta}\eta & -\sinh\bar{\beta}\eta \\ 0 & \sin\bar{\beta}\eta & \cos\bar{\beta}\eta & -\sinh\bar{\beta}\eta & -\cosh\bar{\beta}\eta \end{vmatrix} = 0, \tag{42}$$

where the following non-dimensional parameters are introduced:

$$\bar{\beta} = \beta L_1, \quad \bar{m}_{21} = \frac{m_2 L_2}{m_1 L_1}, \quad \alpha_k = \frac{E_2 A_2/L_2}{48 E_1 I_1/L_1^3}, \quad \alpha_M = \frac{M}{m_1 L_1}, \quad \gamma L_2 = \bar{\beta}^2\sqrt{\bar{m}_{21}/48\alpha_k},$$
$$\alpha_{11} = \frac{\alpha_M}{\sqrt{48\alpha_k\bar{m}_{21}}}, \quad \alpha_{22} = \frac{1}{\sqrt{48\alpha_k\bar{m}_{21}}}. \tag{43}$$

The roots of the transcendental frequency equation above give us the dimensionless frequency parameter $\bar{\beta}$ and therefore by considering Eq. (28), the eigenfrequencies of the system in Fig. 1.

Having obtained the frequency equation of the general system in Fig. 1 it is reasonable to obtain numerical results and make comparisons with those systems which correspond to limit cases of the mechanical system in Fig. 1. Recognizing that $\bar{m}_{21}$ denotes the ratio of the mass of the rod to that of the beam, it is clear that the limit $\bar{m}_{21} \to 0$ corresponds to the simplified system in Fig. 2 for $k = E_2A_2/L_2$. However, it is not possible to obtain it simply by taking the limit $\bar{m}_{21} \to 0$, as expected. The frequency equation of this simplified system can be found in Ref. [9] and is given here in notation of the present paper, with $k = E_2A_2/L_2$:

$$\frac{\sin(\eta\bar{\beta})\sin[(1-\eta)\bar{\beta}]}{\sin\bar{\beta}} - \frac{\sinh(\eta\bar{\beta})\sinh[(1-\eta)\bar{\beta}]}{\sinh\bar{\beta}} = \frac{2}{\bar{\beta}}\left(\frac{\bar{\beta}^4}{48\alpha_k} - \frac{1}{\alpha_M}\right). \tag{44}$$

As the numerical evaluations have shown that the equation above yields accurate results only in the region of small α_M values up to $\alpha_M = 0.1$, the need arose to rederive the frequency equation of the mechanical system in Fig. 2. It is given in Eq. (A.1) directly for the sake of completeness on one side and for the benefit of the design engineers working in this area on the other.

The limit case of $M \to \infty$ corresponds to the system in Fig. 3, derivation of the frequency equation of which will be given in the next section.

2.2. Derivation of the frequency equation of the system in Fig. 3

Unfortunately, it is not possible to obtain the frequency equation of this system from that of the system in Fig. 1 simply by letting $M \to \infty$ in the frequency equation (42). It can be shown that in the previous boundary conditions (14–23), conditions (18) and (20) have to be replaced now by the following expressions, respectively:

$$m_2\int_0^{L_2}[\ddot{w}_2(x_2,t) + \ddot{w}_1(\eta L_1,t)]\,dx_2 - E_1I_1[w_1'''(\eta L_1,t) - w_3'''(\eta L_1,t)] - E_2A_2w_2'(L_2,t) = 0, \tag{45}$$

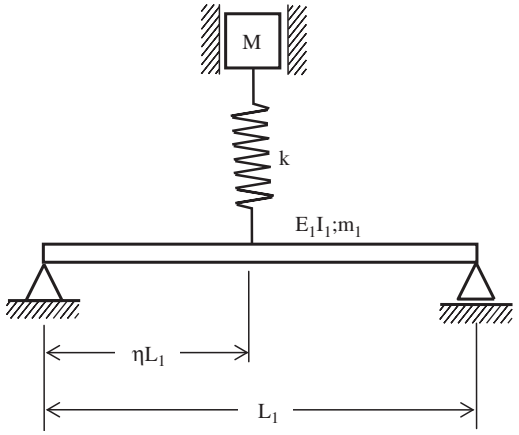

Fig. 2. Vibrational system in Fig. 1 for the limit $\bar{m}_{21} \to 0$.

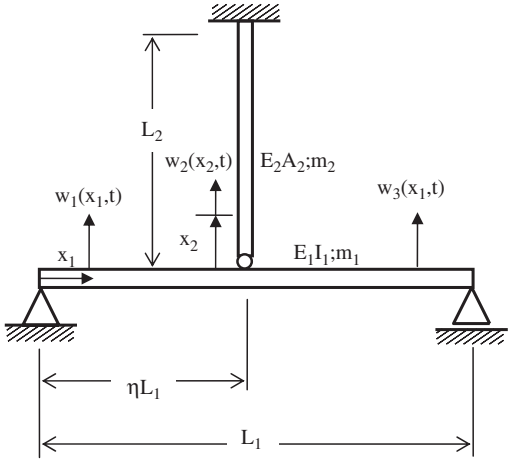

Fig. 3. Vibrational system in Fig. 1 for the limit $\alpha_M \to \infty$.

$$w_2(L_2, t) + w_1(\eta L_1, t) = 0, \tag{46}$$

whereas the remaining conditions are unchanged. The separation solution (24) leads for the amplitude functions to

$$m_2\omega^2 \int_0^{L_2} [W_2(x_2) + W_1(\eta L_1)]\,\mathrm{d}x_2 + E_1 I_1 [W_1'''(\eta L_1) - W_3'''(\eta L_1)] + E_2 A_2 W_2'(L_2) = 0, \tag{47}$$

$$W_2(L_2) + W_1(\eta L_1) = 0. \tag{48}$$

Substitution of Eqs. (39–41) into the boundary conditions yields a set of 10 homogenous equations for the $C_1 - C_{10}$. Setting the corresponding determinant of coefficients to zero, results in the following

frequency equation:

$$\begin{vmatrix} 0 & 1 & 0 & 1 & 0 \\ 0 & 0 & 0 & 0 & 0 \\ 0 & -1 & 0 & 1 & 0 \\ 0 & 0 & 0 & 0 & 0 \\ -\cos\bar{\beta}\eta & \sin\bar{\beta}\eta & \cosh\bar{\beta}\eta & \sinh\bar{\beta}\eta & \dfrac{1}{\bar{\beta}\alpha_{22}}(1-\cos\gamma L_2)+\dfrac{48\alpha_k\gamma L_2}{\bar{\beta}^3}\cos\gamma L_2 \\ -\sin\bar{\beta}\eta & -\cos\bar{\beta}\eta & -\sinh\bar{\beta}\eta & -\cosh\bar{\beta}\eta & 0 \\ 0 & 0 & 0 & 0 & \sin\gamma L_2 \\ \sin\bar{\beta}\eta & \cos\bar{\beta}\eta & \sinh\bar{\beta}\eta & \cosh\bar{\beta}\eta & 0 \\ \cos\bar{\beta}\eta & -\sin\bar{\beta}\eta & \cosh\bar{\beta}\eta & \sinh\bar{\beta}\eta & 0 \\ -\sin\bar{\beta}\eta & -\cos\bar{\beta}\eta & \sinh\bar{\beta}\eta & \cosh\bar{\beta}\eta & 0 \end{vmatrix}$$

$$\begin{vmatrix} 0 & 0 & 0 & 0 & 0 \\ 0 & \sin\bar{\beta} & \cos\bar{\beta} & \sinh\bar{\beta} & \cosh\bar{\beta} \\ 0 & 0 & 0 & 0 & 0 \\ 0 & -\sin\bar{\beta} & -\cos\bar{\beta} & \sinh\bar{\beta} & \cosh\bar{\beta} \\ \dfrac{1}{\bar{\beta}\alpha_{22}}\sin\gamma L_2-\dfrac{48\alpha_k\gamma L_2}{\bar{\beta}^3}\sin\gamma L_2 & \cos\bar{\beta}\eta & -\sin\bar{\beta}\eta & -\cosh\bar{\beta}\eta & -\sinh\bar{\beta}\eta \\ 1 & 0 & 0 & 0 & 0 \\ \cos\gamma L_2 & 0 & 0 & 0 & 0 \\ 0 & -\sin\bar{\beta}\eta & -\cos\bar{\beta}\eta & -\sinh\bar{\beta}\eta & -\cosh\bar{\beta}\eta \\ 0 & -\cos\bar{\beta}\eta & \sin\bar{\beta}\eta & -\cosh\bar{\beta}\eta & -\sinh\bar{\beta}\eta \\ 0 & \sin\bar{\beta}\eta & \cos\bar{\beta}\eta & -\sinh\bar{\beta}\eta & -\cosh\bar{\beta}\eta \end{vmatrix} = 0. \tag{49}$$

For getting trial values for the numerical solution of the transcendental frequency equation (42) on the one hand and for comparison purposes on the other, an approximate formula for the fundamental frequency of the system in Fig. 1 will be derived in the following section.

2.3. *An approximate formula for the fundamental frequency of the system in Fig. 1*

According to Dunkerley's procedure, the mechanical system in Fig. 1 can be thought of the "sum" of three subsystems shown in Fig. 4. The fundamental frequency ω_{11} of the bare simply supported Bernoulli–Euler beam in Fig. 4a is

$$\omega_{11} = \bar{\beta}_{11}^2\sqrt{\frac{E_1 I_1}{m_1 L_1^4}}, \quad \bar{\beta}_{11} = \pi. \tag{50}$$

Making use of the more general expression in Ref. [10], the frequency equation of the second subsystem in Fig. 4b can be shown to be

$$\tan\bar{\beta}_{22} - \frac{1}{16\alpha_k\bar{\beta}_{22}\eta^2(1-\eta)^2} = 0. \tag{51}$$

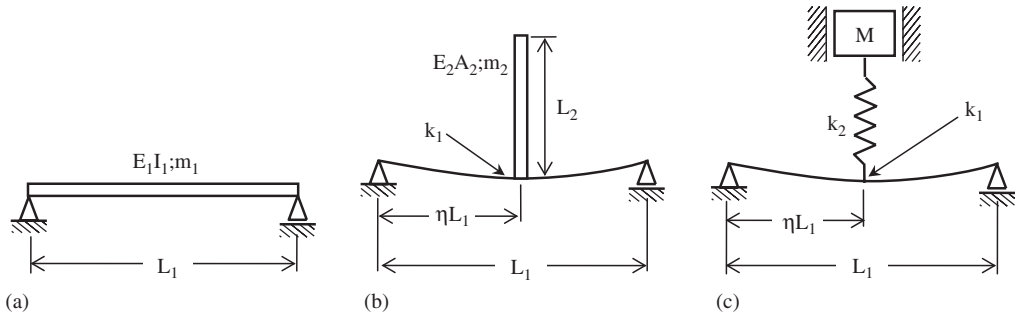

Fig. 4. Partial systems for the application of Dunkerley's procedure.

Once this transcendental equation is solved with respect to the frequency parameter $\bar{\beta}_{22}$, the fundamental frequency ω_{22} of the second system is simply

$$\omega_{22} = \bar{\beta}_{22}\sqrt{\frac{E_2A_2}{m_2L_2^2}}. \tag{52}$$

The eigenfrequency of the third system in Fig. 4c can obtained as

$$\omega_{33} = \sqrt{\frac{k_1k_2}{M(k_1+k_2)}}, \tag{53}$$

where the following spring constants are introduced:

$$k_1 = \frac{3E_1I_1}{\eta^2(1-\eta)^2L_1^3}, \quad k_2 = \frac{E_2A_2}{L_2}. \tag{54-55}$$

According to Dunkerley's method, the approximate value of the fundamental frequency of the system in Fig. 1, ω_1 is obtained via

$$\frac{1}{\omega_1^2} = \frac{1}{\omega_{11}^2} + \frac{1}{\omega_{22}^2} + \frac{1}{\omega_{33}^2}. \tag{56}$$

Substitution of the eigenfrequencies in Eqs. (50), (52) and (53) into Eq. (56) yields after rearrangements

$$\omega_1 = \frac{\bar{\beta}_{11}^2}{\sqrt{1+(\bar{\beta}_{11}^4/\bar{\beta}_{22}^2)(\bar{m}_{21}/48\alpha_k)+\alpha_M\bar{\beta}_{11}^4\left((1/48\alpha_k)+(\eta^2(1-\eta)^2/3)\right)}}\,\omega_0, \tag{57}$$

where

$$\omega_0^2 = \frac{E_1I_1}{m_1L_1^4} \tag{58}$$

is introduced. It is worth noting that $\bar{\beta}_{22}$ represents the first root of Eq. (51) for the corresponding η and α_k values.

It might be thought of deriving also an approximate formula for the fundamental eigenfrequency of the system in Fig. 3 on the basis of the Dunkerley's formula. To this end, the mechanical system in Fig. 3 can be thought of the "sum" of two subsystems shown in Fig. 5. Due to the fact that the fundamental frequencies of both subsystems cannot be given in an analytical form, but instead, can only be obtained numerically, it is not possible to speak of the application of the Dunkerley's formula in the usual sense. Instead, the frequency equation of the system in Fig. 5a is given in Eq. (A.2).

Using the more general formula in Ref. [10], the frequency equation of the system in Fig. 5b can be shown to be

$$\tan\bar{\beta}_{22} + 16\alpha_k\eta^2(1-\eta)^2\bar{\beta}_{22} = 0 \tag{59}$$

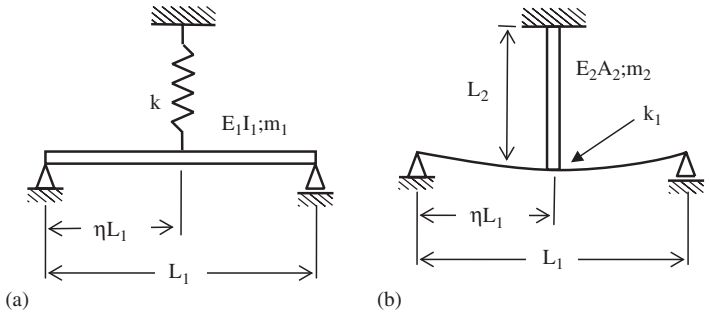

Fig. 5. Subsystems derived from the system in Fig. 3.

with

$$\bar{\beta}_{22} = \beta_{22} L_2, \quad \bar{\beta}_{22}^2 = \frac{\omega^2 m_2 L_2}{E_2 A_2}, \tag{60}$$

where α_k is given previously in Eq. (43).

The roots $\bar{\beta}_{22}$ obtained from Eq. (59) yield via Eq. (60) the eigenfrequencies ω of the system in Fig. 5b. On the other hand, the numerical results obtained from these subsystems constitute via Dunkerley's formula indirectly, valuable trial values for the numerical solution of the frequency equation of the reduced system in Fig. 3 as given in Eq. (49).

3. Numerical results

This section is devoted to the numerical evaluation of the formulas established in the preceding section. Recognizing that $\bar{m}_{21} = 0$ corresponds to the case of the mass of the axially vibrating rod, i.e. helical spring being zero, it is reasonable to make a comparison with the numerical values resulting from the system in Fig. 2.

The non-dimensional fundamental frequency parameters $\bar{\beta}_1$ of the system in Fig. 1 are given in Table 1 for various values of the non-dimensional mass and stiffness parameters α_M, $\bar{m}_{21}$ and α_k, where $\eta = 0.5$ is taken. The values in the first rows indicated by "P" are the numerical values obtained from the numerical solution of the frequency Eq. (42) for $\bar{m}_{21} \to 0$. These are exactly the same results as those obtained from the frequency equation corresponding to the mechanical system in Fig. 2, i.e. Eq. (A.1). The rows indicated by "F" are the results obtained from a finite elements package FINES [11] and rows indicated by "D" are derived via Dunkerley-based formula (57). For $\bar{m}_{21} = 0.01$ and 0.1, the values of $\bar{\beta}_1$ obtained from Eq. (42), FINES and Eq. (58) are given in the following rows of Table 1. All numerical calculations were carried out with MATLAB. In the FE solutions, each of the beam and the rod were modeled using 10 elements.

As expected, the values given in the third rows of each cell which are based on Dunkerley's formula, are smaller than those in the first rows, indeed, it is a known fact that the Dunkerley-based values are always smaller than the actual values. These values constitute very suitable initial values for the numerical solution of the transcendental Eq. (42) from which the first row values are obtained.

It is natural that the values for $\bar{m}_{21} = 0.01$ are smaller than the values which correspond to the massless spring case, because these correspond to the case with the spring with mass. On the other hand, the values for $\bar{m}_{21} = 0.1$ are smaller than the values for $\bar{m}_{21} = 0.01$, because the spring mass is 10 times.

The absolute values of the relative "errors" of the "P" values for the $\bar{m}_{21} = 0$-case, with respect to the "P" values for $\bar{m}_{21} = 0.01$ and 0.1, respectively are given separately in Fig. 6. The error surfaces are shown in Fig. 6 from bottom to top for $\bar{m}_{21} = 0.01$ and 0.1, respectively. It is seen that the error values grow linearly with $\bar{m}_{21}$, for example, the error values corresponding to $\bar{m}_{21} = 0.1$ are approximately 10 times larger than those corresponding to $\bar{m}_{21} = 0.01$.

Further, Fig. 6 reveals the fact that errors get smaller if one moves along the α_M axis, i.e., if α_M gets larger by holding α_k constant. On the other side, if α_k gets larger by keeping α_M fixed, the errors get slightly larger, as well.

Table 1
Non-dimensional fundamental frequency parameters $\bar{\beta}_1$ of the system in Fig. 1 for various values of the stiffness and mass parameters α_k, α_M and $\bar{m}_{21}$, where $\eta = 0.5$ is taken

α_M	$\bar{m}_{21}$		α_k							
			0.5	1	1.5	2	2.5	3	5	10
0.5	0	*P*	2.304807	2.464754	2.523090	2.552556	2.570202	2.581918	2.605164	2.622368
		F	2.304808	2.464756	2.523092	2.552558	2.570204	2.581921	2.605166	2.622370
		D	2.215370	2.381290	2.452823	2.492946	2.518671	2.536582	2.574414	2.604735
	0.01	*P*	2.299620	2.458815	2.516891	2.546237	2.563815	2.575489	2.598656	2.615808
		F	2.299621	2.458816	2.516893	2.546239	2.563817	2.575491	2.598658	2.615811
		D	2.210602	2.375932	2.447165	2.487105	2.512706	2.530528	2.568165	2.598320
	0.1	*P*	2.254997	2.408078	2.464083	2.492474	2.509521	2.520861	2.543419	2.560169
		F	2.255002	2.408082	2.464087	2.492478	2.509524	2.520865	2.543422	2.560171
		D	2.169873	2.330265	2.399002	2.437426	2.462007	2.479096	2.515119	2.543915
1	0	*P*	1.970968	2.143717	2.215896	2.255032	2.279459	2.296118	2.330261	2.356506
		F	1.970969	2.143718	2.215897	2.255033	2.279460	2.296119	2.330262	2.356507
		D	1.925386	2.094787	2.171328	2.215370	2.244068	2.264275	2.307603	2.343000
	0.01	*P*	1.968651	2.140823	2.212706	2.251669	2.275984	2.292565	2.326543	2.352658
		F	1.968652	2.140824	2.212707	2.251670	2.275985	2.292566	2.326544	2.352659
		D	1.923017	2.091958	2.168245	2.212125	2.240712	2.260837	2.303979	2.339214
	0.1	*P*	1.948259	2.115502	2.184894	2.222403	2.245778	2.261705	2.294315	2.319357
		F	1.948261	2.115503	2.184895	2.222405	2.245780	2.261706	2.294316	2.319358
		D	1.902326	2.067328	2.141448	2.183954	2.211590	2.231019	2.272591	2.306461
1.5	0	*P*	1.790122	1.958421	2.032281	2.073575	2.099871	2.118056	2.156012	2.185862
		F	1.790122	1.958422	2.032282	2.073576	2.099872	2.118056	2.156013	2.185863
		D	1.760861	1.925386	2.001207	2.045329	2.074290	2.094787	2.139047	2.175538
	0.01	*P*	1.788705	1.956604	2.030237	2.071388	2.097586	2.115700	2.153503	2.183224
		F	1.788705	1.956605	2.030237	2.071389	2.097587	2.115701	2.153504	2.183225
		D	1.759343	1.923529	1.999155	2.043150	2.072023	2.094721	2.136564	2.172922
	0.1	*P*	1.776138	1.940556	2.012229	2.052153	2.077519	2.095034	2.131526	2.160160
		F	1.776139	1.940557	2.012230	2.052154	2.077520	2.095035	2.131527	2.160161
		D	1.745974	1.907205	1.981147	2.024051	2.052161	2.072028	2.114849	2.150067
2	0	*P*	1.670013	1.832352	1.905377	1.946881	1.973611	1.992245	2.031574	2.062949
		F	1.670014	1.832352	1.905377	1.946882	1.973612	1.992246	2.031575	2.062950
		D	1.648932	1.807931	1.882007	1.925386	1.953980	1.974277	2.018282	2.054758
	0.01	*P*	1.669018	1.831059	1.903907	1.945296	1.971945	1.990521	2.029716	2.060978
		F	1.669018	1.831060	1.903908	1.945297	1.971946	1.990521	2.029717	2.060978
		D	1.647839	1.806574	1.880497	1.923775	1.952297	1.972541	2.016425	2.052791
	0.1	*P*	1.660155	1.819590	1.890895	1.931283	1.957236	1.975302	2.013352	2.043632
		F	1.660156	1.819591	1.890896	1.931284	1.957237	1.975302	2.013353	2.043633
		D	1.638161	1.794589	1.867170	1.909570	1.937473	1.957256	2.000080	2.035501
2.5	0	*P*	1.581695	1.738471	1.810043	1.851138	1.877794	1.896474	1.936190	1.968184
		F	1.581695	1.738471	1.810043	1.851138	1.877794	1.896474	1.936190	1.968185
		D	1.565439	1.719343	1.791542	1.833994	1.862052	1.882007	1.925386	1.961469
	0.01	*P*	1.580938	1.737482	1.808912	1.849912	1.876501	1.895131	1.934733	1.966627
		F	1.580939	1.737483	1.808912	1.849913	1.876501	1.895132	1.934734	1.966628
		D	1.564595	1.718287	1.790361	1.832731	1.860729	1.880640	1.923918	1.959909
	0.1	*P*	1.574193	1.728686	1.798866	1.839038	1.865042	1.883239	1.921852	1.952880
		F	1.574194	1.728687	1.798867	1.839039	1.865043	1.883240	1.921853	1.952880
		D	1.557106	1.708930	1.779904	1.821547	1.849032	1.868559	1.910950	1.946144

Table 1 (*continued*)

α_M	$\bar{m}_{21}$		α_k							
			0.5	1	1.5	2	2.5	3	5	10
3	0	*P*	1.512662	1.664519	1.734528	1.775003	1.801387	1.819945	1.859604	1.891777
		F	1.512663	1.664519	1.734528	1.775004	1.801388	1.819945	1.859605	1.891778
		D	1.499554	1.648932	1.719343	1.760861	1.788352	1.807931	1.850572	1.886128
	0.01	*P*	1.512059	1.663726	1.733617	1.774013	1.800340	1.818855	1.858416	1.890501
		F	1.512059	1.663727	1.733618	1.774014	1.800341	1.818856	1.858417	1.890502
		D	1.498874	1.648076	1.718381	1.759829	1.787271	1.806813	1.849368	1.884846
	0.1	*P*	1.506667	1.656661	1.725513	1.765210	1.791038	1.809181	1.847882	1.879203
		F	1.506668	1.656661	1.725513	1.765211	1.791039	1.809181	1.847883	1.879203
		D	1.492819	1.640464	1.709845	1.750679	1.777685	1.796900	1.838698	1.873493
5	0	*P*	1.333816	1.471095	1.535627	1.573463	1.598380	1.616040	1.654204	1.685641
		F	1.333816	1.471095	1.535628	1.573464	1.598380	1.616041	1.654204	1.685642
		D	1.326716	1.462473	1.527102	1.565439	1.590925	1.609128	1.648932	1.682300
	0.01	*P*	1.333496	1.470671	1.535136	1.572926	1.597808	1.615443	1.653545	1.684926
		F	1.333496	1.470671	1.535137	1.572926	1.597809	1.615443	1.653546	1.684927
		D	1.326347	1.462002	1.526570	1.564865	1.590322	1.608503	1.648255	1.681575
	0.1	*P*	1.330628	1.466876	1.530745	1.568122	1.592704	1.610110	1.647673	1.678558
		F	1.330628	1.466876	1.530745	1.568122	1.592704	1.610111	1.647674	1.678559
		D	1.323050	1.457803	1.521825	1.559754	1.584949	1.602932	1.642223	1.675124
10	0	*P*	1.123153	1.240869	1.297010	1.330280	1.352363	1.368112	1.402451	1.431100
		F	1.123154	1.240870	1.297011	1.330280	1.352364	1.368112	1.402452	1.431101
		D	1.120111	1.237115	1.293256	1.326716	1.349033	1.365009	1.400057	1.429566
	0.01	*P*	1.123018	1.240689	1.296801	1.330049	1.352117	1.367853	1.402164	1.430786
		F	1.123019	1.240690	1.296801	1.330049	1.352118	1.367854	1.402165	1.430786
		D	1.119953	1.236911	1.293024	1.326466	1.348768	1.364734	1.399758	1.429245
	0.1	*P*	1.121806	1.239074	1.294920	1.327980	1.349909	1.365539	1.399592	1.427970
		F	1.121806	1.239075	1.294920	1.327980	1.349910	1.365539	1.399592	1.427970
		D	1.118533	1.235085	1.290948	1.324220	1.346401	1.362274	1.397082	1.426370

The values in the first rows indicated by "P" are frequency parameters obtained from the solution of Eq. (42). The rows indicated by "F" are the results obtained from FINES and the rows indicated by "D" are from the Dunkerley-based formula (57).

The interesting fact depicted by Fig. 6 is that neglecting the mass of the helical spring represented in Fig. 1 by the axially vibrating rod results in larger errors, especially in the small α_M and large α_k regions.

As a second numerical application, the fundamental eigenfrequency parameters $\bar{\beta}_1$ of the system in Fig. 3 are collected in Table 2 for various values of the stiffness parameter α_k, where $\eta = 0.5$ is taken again. The values in the first rows are obtained from Eq. (A.2), corresponding to $\bar{m}_{21} = 0$. The next two values correspond to $\bar{m}_{21} = 0.01$ and 0.1, respectively. The relative errors of the $\bar{m}_{21} = 0$-case with respect to these values are given right shifted above them. As before, the error values corresponding to $\bar{m}_{21} = 0.1$ are approximately 10 times larger than those corresponding to $\bar{m}_{21} = 0.01$.

It is clearly seen from Table 2 that the mass of helical spring affects the numerical values of the frequency parameters. The consideration of the own mass of the helical spring leads to smaller frequency parameters, as expected. The remaining three values are FINES-based solutions corresponding to $\bar{m}_{21} = 0$, 0.01 and 0.1, respectively. It is reasonable that the FINES-based values are somewhat larger than those for $\bar{m}_{21} = 0$. Table 2 reveals clearly that errors resulting from not considering the own mass of the helical spring get smaller if α_k gets larger which represents a contrary trend to that seen in Fig. 6.

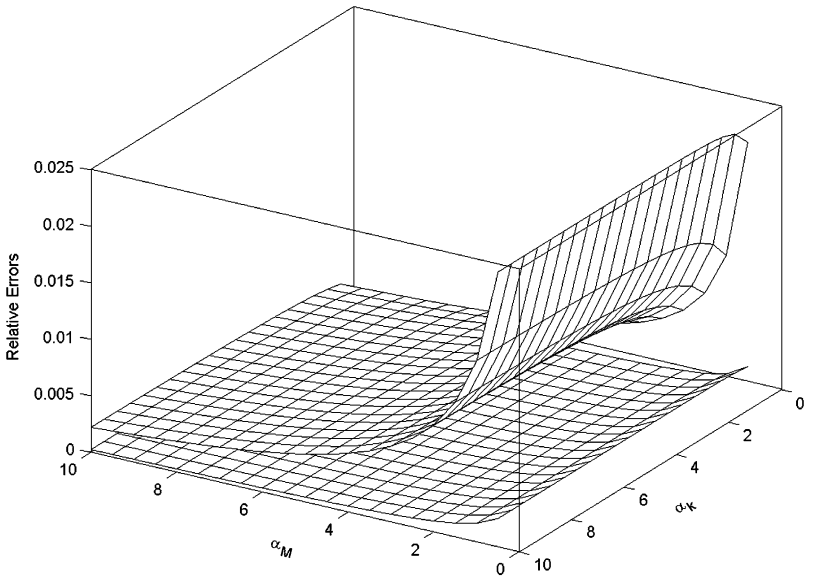

Fig. 6. The relative "errors" of the $\bar{m}_{21} = 0$-case with respect to the "P" values in each cell for various values of the stiffness and mass parameters α_k, α_M and $\bar{m}_{21}$, where $\eta = 0.5$ is taken. The lower and upper surfaces correspond to $\bar{m}_{21} = 0.01$ and 0.1, respectively.

Table 2
Non-dimensional fundamental frequency parameters $\bar{\beta}_1$ of the system in Fig. 3 for various values of the stiffness and mass parameters α_k and $\bar{m}_{21}$, where $\eta = 0.5$ is taken

α_k 0.5	1	1.5	2	2.5	3	5	10
3.470452	3.722474	3.928871	4.104587	4.258048	4.394514	4.827545	5.513735
−0.001642	−0.001616	−0.001592	−0.001568	−0.001544	−0.001521	−0.001430	−0.001218
3.464752	3.716457	3.922617	4.098152	4.251472	4.387831	4.820643	5.507019
−0.016407	−0.015975	−0.015687	−0.015435	−0.015198	−0.014969	−0.014098	−0.012092
3.413511	3.663008	3.867240	4.041234	4.193334	4.328731	4.759488	5.447061
3.470470	3.722499	3.928905	4.104629	4.258097	4.394571	4.827636	5.513912
3.464770	3.716482	3.922650	4.098193	4.251520	4.387887	4.820733	5.507194
3.413553	3.663049	3.867284	4.041284	4.193391	4.328794	4.759580	5.447229

The values in the first rows are obtained from equation (A2), corresponding to $\bar{m}_{21} = 0$. The next two values correspond to $\bar{m}_{21} = 0.01$ and 0.1. The right shifted values above them are the relative "errors" of the $\bar{m}_{21} = 0$-case with respect to these values. The last three values are FINES-based solutions corresponding to $\bar{m}_{21} = 0$, 0.01 and 0.1, respectively.

4. Conclusion

Many actual systems in the real life are modeled in the technical literature as Bernoulli–Euler beams subject to various supporting conditions with helical spring–mass additions. However, in these applications the helical springs are frequently assumed to be massless. The system investigated in the present study is made up of a simply supported beam to which a helical spring–mass is attached in-span. In order to account for the own mass of the helical spring, it is modeled as a longitudinally vibrating elastic rod. The frequency equation of the above-combined system is derived. Further, the frequency equation of the reduced system resulting for the tip mass going to infinity is established as well. The frequency equations obtained are then numerically solved for

various combinations of the physical parameters. Comparison of the numerical results with the massless spring case reveals the fact that neglecting the mass causes considerable errors for some combinations of the physical parameters and thus, it is quite reasonable to consider the mass of the helical springs in order to obtain more realistic eigenfrequencies of the combined system.

Appendix A

$$
\begin{vmatrix}
0 & 1 & 0 & 1 & 0 \\
0 & -1 & 0 & 1 & 0 \\
0 & 0 & 0 & 0 & \sin\bar{\beta} \\
0 & 0 & 0 & 0 & -\sin\bar{\beta} \\
\sin\bar{\beta}\eta & \cos\bar{\beta}\eta & \sinh\bar{\beta}\eta & \cosh\bar{\beta}\eta & 0 \\
\sin\bar{\beta}\eta & \cos\bar{\beta}\eta & \sinh\bar{\beta}\eta & \cosh\bar{\beta}\eta & -\sin\bar{\beta}\eta \\
\cos\bar{\beta}\eta & -\sin\bar{\beta}\eta & \cosh\bar{\beta}\eta & \sinh\bar{\beta}\eta & -\cos\bar{\beta}\eta \\
-\sin\bar{\beta}\eta & -\cos\bar{\beta}\eta & \sinh\bar{\beta}\eta & \cosh\bar{\beta}\eta & \sin\bar{\beta}\eta \\
-\cos\bar{\beta}\eta & \sin\bar{\beta}\eta & \cosh\bar{\beta}\eta & \sinh\bar{\beta}\eta & \cos\bar{\beta}\eta
\end{vmatrix}
\begin{vmatrix}
0 & 0 & 0 & 0 \\
0 & 0 & 0 & 0 \\
\cos\bar{\beta} & \sinh\bar{\beta} & \cosh\bar{\beta} & 0 \\
-\cos\bar{\beta} & \sinh\bar{\beta} & \cosh\bar{\beta} & 0 \\
0 & 0 & 0 & -1+\frac{\alpha_M}{48\tilde{z}_k}\bar{\beta}^4 \\
-\cos\bar{\beta}\eta & -\sinh\bar{\beta}\eta & -\cosh\bar{\beta}\eta & 0 \\
\sin\bar{\beta}\eta & -\cosh\bar{\beta}\eta & -\sinh\bar{\beta}\eta & 0 \\
\cos\bar{\beta}\eta & -\sinh\bar{\beta}\eta & -\cosh\bar{\beta}\eta & 0 \\
-\sin\bar{\beta}\eta & -\cosh\bar{\beta}\eta & -\sinh\bar{\beta}\eta & \alpha_M\bar{\beta}
\end{vmatrix} = 0. \tag{A.1}
$$

$$
\begin{vmatrix}
0 & 1 & 0 & 1 \\
0 & -1 & 0 & 1 \\
0 & 0 & 0 & 0 \\
0 & 0 & 0 & 0 \\
\sin\bar{\beta}\eta & \cos\bar{\beta}\eta & \sinh\bar{\beta}\eta & \cosh\bar{\beta}\eta \\
\cos\bar{\beta}\eta & -\sin\bar{\beta}\eta & \cosh\bar{\beta}\eta & \sinh\bar{\beta}\eta \\
-\sin\bar{\beta}\eta & -\cos\bar{\beta}\eta & \sinh\bar{\beta}\eta & \cosh\bar{\beta}\eta \\
-\cos\bar{\beta}\eta - \frac{48\tilde{z}_k}{\bar{\beta}^3}\sin\bar{\beta}\eta & \sin\bar{\beta}\eta - \frac{48\tilde{z}_k}{\bar{\beta}^3}\cos\bar{\beta}\eta & \cosh\bar{\beta}\eta - \frac{48\tilde{z}_k}{\bar{\beta}^3}\sinh\bar{\beta}\eta & \sinh\bar{\beta}\eta - \frac{48\tilde{z}_k}{\bar{\beta}^3}\cosh\bar{\beta}\eta
\end{vmatrix}
$$

$$\begin{vmatrix} 0 & 0 & 0 & 0 \\ 0 & 0 & 0 & 0 \\ \sin\bar{\beta} & \cos\bar{\beta} & \sinh\bar{\beta} & \cosh\bar{\beta} \\ -\sin\bar{\beta} & -\cos\bar{\beta} & \sinh\bar{\beta} & \cosh\bar{\beta} \\ -\sin\bar{\beta}\eta & -\cos\bar{\beta}\eta & -\sinh\bar{\beta}\eta & -\cosh\bar{\beta}\eta \\ -\cos\bar{\beta}\eta & \sin\bar{\beta}\eta & -\cosh\bar{\beta}\eta & -\sinh\bar{\beta}\eta \\ \sin\bar{\beta}\eta & \cos\bar{\beta}\eta & -\sinh\bar{\beta}\eta & -\cosh\bar{\beta}\eta \\ \cos\bar{\beta}\eta & -\sin\bar{\beta}\eta & -\cosh\bar{\beta}\eta & -\sinh\bar{\beta}\eta \end{vmatrix} = 0, \tag{A.2}$$

where $\bar{\alpha}_k = k/(48E_1I_1/L_1^3)$ is introduced.

References

[1] M. Gürgöze, On the eigenfrequencies of a cantilever beam with attached tip mass and a spring–mass system, *Journal of Sound and Vibration* 190 (1996) 149–162.

[2] H. Qiao, Q.S. Li, G.O. Li, Vibratory characteristic of non-uniform Euler–Bernoulli beams carrying an arbitrary number of spring–mass systems, *International Journal of Mechanical Sciences* 44 (2002) 725–743.

[3] J.-J. Wu, Alternative approach for free vibration of beams carrying a number of two-degree of freedom spring–mass systems, *Journal of Structural Engineering* 128 (2002) 1604–1616.

[4] D.-W. Chen, J.-S. Wu, The exact solutions for the natural frequencies and mode shapes of non-uniform beams with multiple spring–mass systems, *Journal of Sound and Vibration* 255 (2002) 229–232.

[5] M. Gürgöze, Comments on a technical note by C.A. Rossi and P.A.A. Laura, *Ocean Engineering* 29 (2002) 299–302.

[6] M. Gürgöze, On the eigenfrequencies of cantilevered beams carrying a tip mass and spring–mass in-span, *International Journal of Mechanical Sciences* 38 (12) (1996) 1295–1306.

[7] M. Gürgöze, On the eigenfrequencies of a cantilever beam carrying a tip spring–mass system with mass of the helical spring considered, *Journal of Sound and Vibration* 282 (2005) 1221–1230.

[8] M.L. James, G.M. Smith, J.C. Wolford, P.W. Whaley, *Vibration of Mechanical and Structural Systems*, HarperCollins College Publishers, New York, 1994.

[9] B.N. Omid, J.L. Sackman, A.D. Kiureghian, Modal characterization of equipment-continuous structure systems, *Journal of Sound and Vibration* 88 (1983) 459–472.

[10] P.A.A. Laura, J.A. Reyes, R.E. Rossi, Analysis of a cable-like system suddenly stopped at one end, *Journal of Sound and Vibration* 37 (1974) 195–204.

[11] K.Y. Şanlıtürk, *FINES: Finite Element for Structures*, Version 2004, Istanbul Technical University, Mechanical Engineering Department, Istanbul, Turkey.